

Observation of Direct-Photon Collective Flow in Au + Au Collisions at $\sqrt{s_{NN}} = 200$ GeV

A. Adare,¹¹ S. Afanasiev,²⁷ C. Aidala,³⁹ N.N. Ajitanand,⁵⁶ Y. Akiba,^{50,51} H. Al-Bataineh,⁴⁵ J. Alexander,⁵⁶ K. Aoki,^{32,50} Y. Aramaki,¹⁰ E. T. Atomssa,³³ R. Averbeck,⁵⁷ T. C. Awes,⁴⁶ B. Azmoun,⁵ V. Babintsev,²² M. Bai,⁴ G. Baksay,¹⁸ L. Baksay,¹⁸ K. N. Barish,⁶ B. Bassalleck,⁴⁴ A. T. Basye,¹ S. Bathe,⁶ V. Baublis,⁴⁹ C. Baumann,⁴⁰ A. Bazilevsky,⁵ S. Belikov,^{5,*} R. Belmont,⁶¹ R. Bennett,⁵⁷ A. Berdnikov,⁵³ Y. Berdnikov,⁵³ A. A. Bickley,¹¹ J. S. Bok,⁶⁵ K. Boyle,⁵⁷ M. L. Brooks,³⁵ H. Buesching,⁵ V. Bumazhnov,²² G. Bunce,^{5,51} S. Butsyk,³⁵ C. M. Camacho,³⁵ S. Campbell,⁵⁷ C.-H. Chen,⁵⁷ C. Y. Chi,¹² M. Chiu,⁵ I. J. Choi,⁶⁵ R. K. Choudhury,³ P. Christiansen,³⁷ T. Chujo,⁶⁰ P. Chung,⁵⁶ O. Chvala,⁶ V. Cianciolo,⁴⁶ Z. Citron,⁵⁷ B. A. Cole,¹² M. Connors,⁵⁷ P. Constantin,³⁵ M. Csanád,¹⁶ T. Csörgő,⁶⁴ T. Dahms,⁵⁷ S. Dairaku,^{32,50} I. Danchev,⁶¹ K. Das,¹⁹ A. Datta,³⁹ G. David,⁵ A. Denisov,²² A. Deshpande,^{51,57} E. J. Desmond,⁵ O. Dietzsch,⁵⁴ A. Dion,⁵⁷ M. Donadelli,⁵⁴ O. Drapier,³³ A. Drees,⁵⁷ K. A. Drees,⁴ J. M. Durham,⁵⁷ A. Durum,²² D. Dutta,³ S. Edwards,¹⁹ Y. V. Efremenko,⁴⁶ F. Ellinghaus,¹¹ T. Engelmore,¹² A. Enokizono,³⁴ H. En'yo,^{50,51} S. Esumi,⁶⁰ B. Fadem,⁴¹ D. E. Fields,⁴⁴ M. Finger,⁷ M. Finger, Jr.,⁷ F. Fleuret,³³ S. L. Fokin,³¹ Z. Fraenkel,^{63,*} J. E. Frantz,⁵⁷ A. Franz,⁵ A. D. Frawley,¹⁹ K. Fujiwara,⁵⁰ Y. Fukao,⁵⁰ T. Fusayasu,⁴³ I. Garishvili,⁵⁸ A. Glenn,¹¹ H. Gong,⁵⁷ M. Gonin,³³ Y. Goto,^{50,51} R. Granier de Cassagnac,³³ N. Grau,¹² S. V. Greene,⁶¹ M. Grosse Perdekamp,^{23,51} T. Gunji,¹⁰ H.-Å. Gustafsson,^{37,*} J. S. Haggerty,⁵ K. I. Hahn,¹⁷ H. Hamagaki,¹⁰ J. Hamblen,⁵⁸ R. Han,⁴⁸ J. Hanks,¹² E. P. Hartouni,³⁴ E. Haslum,³⁷ R. Hayano,¹⁰ X. He,²⁰ M. Heffner,³⁴ T. K. Hemmick,⁵⁷ T. Hester,⁶ J. C. Hill,²⁶ M. Hohlmann,¹⁸ W. Holzmann,¹² K. Homma,²¹ B. Hong,³⁰ T. Horaguchi,²¹ D. Hornback,⁵⁸ S. Huang,⁶¹ T. Ichihara,^{50,51} R. Ichimiya,⁵⁰ J. Ide,⁴¹ Y. Ikeda,⁶⁰ K. Imai,^{32,50} M. Inaba,⁶⁰ D. Isenhower,¹ M. Ishihara,⁵⁰ T. Isobe,^{10,50} M. Issah,⁶¹ A. Isupov,²⁷ D. Ivanishev,⁴⁹ B. V. Jacak,^{57,†} J. Jia,^{5,56} J. Jin,¹² B. M. Johnson,⁵ K. S. Joo,⁴² D. Jouan,⁴⁷ D. S. Jumper,¹ F. Kajihara,¹⁰ S. Kametani,⁵⁰ N. Kamihara,⁵¹ J. Kamin,⁵⁷ J. H. Kang,⁶⁵ J. Kapustinsky,³⁵ K. Karatsu,^{32,50} D. Kawall,^{39,51} M. Kawashima,^{50,52} A. V. Kazantsev,³¹ T. Kempel,²⁶ A. Khanzadeev,⁴⁹ K. M. Kijima,²¹ B. I. Kim,³⁰ D. H. Kim,⁴² D. J. Kim,²⁸ E. Kim,⁵⁵ E. J. Kim,⁸ S. H. Kim,⁶⁵ Y. J. Kim,²³ E. Kinney,¹¹ K. Kiriluk,¹¹ Á. Kiss,¹⁶ E. Kistenev,⁵ C. Klein-Boesing,⁴⁰ L. Kochenda,⁴⁹ B. Komkov,⁴⁹ M. Konno,⁶⁰ J. Koster,²³ D. Kotchetkov,⁴⁴ A. Kozlov,⁶³ A. Král,¹³ A. Kravitz,¹² G. J. Kunde,³⁵ K. Kurita,^{50,52} M. Kurosawa,⁵⁰ Y. Kwon,⁶⁵ G. S. Kyle,⁴⁵ R. Lacey,⁵⁶ Y. S. Lai,¹² J. G. Lajoie,²⁶ A. Lebedev,²⁶ D. M. Lee,³⁵ J. Lee,¹⁷ K. Lee,⁵⁵ K. B. Lee,³⁰ K. S. Lee,³⁰ M. J. Leitch,³⁵ M. A. L. Leite,⁵⁴ E. Leitner,⁶¹ B. Lenzi,⁵⁴ X. Li,⁹ P. Liebing,⁵¹ L. A. Linden Levy,¹¹ T. Liška,¹³ A. Litvinenko,²⁷ H. Liu,^{35,45} M. X. Liu,³⁵ B. Love,⁶¹ R. Luechtenborg,⁴⁰ D. Lynch,⁵ C. F. Maguire,⁶¹ Y. I. Makdisi,⁴ A. Malakhov,²⁷ M. D. Malik,⁴⁴ V. I. Manko,³¹ E. Mannel,¹² Y. Mao,^{48,50} H. Masui,⁶⁰ F. Matathias,¹² M. McCumber,⁵⁷ P. L. McGaughey,³⁵ N. Means,⁵⁷ B. Meredith,²³ Y. Miake,⁶⁰ A. C. Mignerey,³⁸ P. Mikeš,^{7,25} K. Miki,^{50,60} A. Milov,⁵ M. Mishra,² J. T. Mitchell,⁵ A. K. Mohanty,³ Y. Morino,¹⁰ A. Morreale,⁶ D. P. Morrison,⁵ T. V. Moukhanova,³¹ J. Murata,^{50,52} S. Nagamiya,²⁹ J. L. Nagle,¹¹ M. Naglis,⁶³ M. I. Nagy,¹⁶ I. Nakagawa,^{50,51} Y. Nakamiya,²¹ T. Nakamura,^{21,29} K. Nakano,^{50,59} J. Newby,³⁴ M. Nguyen,⁵⁷ R. Nouicer,⁵ A. S. Nyanin,³¹ E. O'Brien,⁵ S. X. Oda,¹⁰ C. A. Ogilvie,²⁶ M. Oka,⁶⁰ K. Okada,⁵¹ Y. Onuki,⁵⁰ A. Oskarsson,³⁷ M. Ouchida,^{21,50} K. Ozawa,¹⁰ R. Pak,⁵ V. Pantuev,^{24,57} V. Papavassiliou,⁴⁵ I. H. Park,¹⁷ J. Park,⁵⁵ S. K. Park,³⁰ W. J. Park,³⁰ S. F. Pate,⁴⁵ H. Pei,²⁶ J.-C. Peng,²³ H. Pereira,¹⁴ V. Peresedov,²⁷ D. Yu. Peressounko,³¹ C. Pinkenburg,⁵ R. P. Pisani,⁵ M. Proissl,⁵⁷ M. L. Purschke,⁵ A. K. Purwar,³⁵ H. Qu,²⁰ J. Rak,²⁸ A. Rakotozafindrabe,³³ I. Ravinovich,⁶³ K. F. Read,^{46,58} K. Reygers,⁴⁰ V. Riabov,⁴⁹ Y. Riabov,⁴⁹ E. Richardson,³⁸ D. Roach,⁶¹ G. Roche,³⁶ S. D. Rolnick,⁶ M. Rosati,²⁶ C. A. Rosen,¹¹ S. S. E. Rosendahl,³⁷ P. Rosnet,³⁶ P. Rukoyatkin,²⁷ P. Ružička,²⁵ B. Sahlmueller,⁴⁰ N. Saito,²⁹ T. Sakaguchi,⁵ K. Sakashita,^{50,59} V. Samsonov,⁴⁹ S. Sano,^{10,62} T. Sato,⁶⁰ S. Sawada,²⁹ K. Sedgwick,⁶ J. Seele,¹¹ R. Seidl,²³ A. Yu. Semenov,²⁶ R. Seto,⁶ D. Sharma,⁶³ I. Shein,²² T.-A. Shibata,^{50,59} K. Shigaki,²¹ M. Shimomura,⁶⁰ K. Shoji,^{32,50} P. Shukla,³ A. Sickles,⁵ C. L. Silva,⁵⁴ D. Silvermyr,⁴⁶ C. Silvestre,¹⁴ K. S. Sim,³⁰ B. K. Singh,² C. P. Singh,² V. Singh,² M. Slunečka,⁷ R. A. Soltz,³⁴ W. E. Sondheim,³⁵ S. P. Sorensen,⁵⁸ I. V. Sourikova,⁵ N. A. Sparks,¹ P. W. Stankus,⁴⁶ E. Stenlund,³⁷ S. P. Stoll,⁵ T. Sugitate,²¹ A. Sukhanov,⁵ J. Sziklai,⁶⁴ E. M. Takagui,⁵⁴ A. Taketani,^{50,51} R. Tanabe,⁶⁰ Y. Tanaka,⁴³ K. Tanida,^{32,50,51} M. J. Tannenbaum,⁵ S. Tarafdar,² A. Taranenko,⁵⁶ P. Tarján,¹⁵ H. Themann,⁵⁷ T. L. Thomas,⁴⁴ M. Togawa,^{32,50} A. Toia,⁵⁷ L. Tomášek,²⁵ H. Torii,²¹ R. S. Towell,¹ I. Tserruya,⁶³ Y. Tsuchimoto,²¹ C. Vale,^{5,26} H. Valle,⁶¹ H. W. van Hecke,³⁵ E. Vazquez-Zambrano,¹² A. Veicht,²³ J. Velkova,⁶¹ R. Vértesi,^{15,64} A. A. Vinogradov,³¹ M. Virius,¹³ V. Vrba,²⁵ E. Vznuzdaev,⁴⁹ X. R. Wang,⁴⁵ D. Watanabe,²¹ K. Watanabe,⁶⁰ Y. Watanabe,^{50,51} F. Wei,²⁶ R. Wei,⁵⁶ J. Wessels,⁴⁰ S. N. White,⁵ D. Winter,¹² J. P. Wood,¹ C. L. Woody,⁵ R. M. Wright,¹ M. Wysocki,¹¹ W. Xie,⁵¹ Y. L. Yamaguchi,¹⁰ K. Yamaura,²¹ R. Yang,²³ A. Yanovich,²² J. Ying,²⁰ S. Yokkaichi,^{50,51} Z. You,⁴⁸ G. R. Young,⁴⁶ I. Younus,⁴⁴ I. E. Yushmanov,³¹ W. A. Zajc,¹² C. Zhang,⁴⁶ S. Zhou,⁹ and L. Zolin²⁷

(PHENIX Collaboration)

- ¹Abilene Christian University, Abilene, Texas 79699, USA
²Department of Physics, Banaras Hindu University, Varanasi 221005, India
³Bhabha Atomic Research Centre, Bombay 400 085, India
⁴Collider-Accelerator Department, Brookhaven National Laboratory, Upton, New York 11973-5000, USA
⁵Physics Department, Brookhaven National Laboratory, Upton, New York 11973-5000, USA
⁶University of California-Riverside, Riverside, California 92521, USA
⁷Charles University, Ovocný trh 5, Praha 1, 116 36, Prague, Czech Republic
⁸Chonbuk National University, Jeonju, 561-756, Korea
⁹Science and Technology on Nuclear Data Laboratory, China Institute of Atomic Energy, Beijing 102413, People's Republic of China
¹⁰Center for Nuclear Study, Graduate School of Science, University of Tokyo, 7-3-1 Hongo, Bunkyo, Tokyo 113-0033, Japan
¹¹University of Colorado, Boulder, Colorado 80309, USA
¹²Columbia University, New York, New York 10027 and Nevis Laboratories, Irvington, New York 10533, USA
¹³Czech Technical University, Zikova 4, 166 36 Prague 6, Czech Republic
¹⁴Dapnia, CEA Saclay, F-91191, Gif-sur-Yvette, France
¹⁵Debrecen University, H-4010 Debrecen, Egyetem tér 1, Hungary
¹⁶ELTE, Eötvös Loránd University, H-1117 Budapest, Pázmány P. s. 1/A, Hungary
¹⁷Ewha Womans University, Seoul 120-750, Korea
¹⁸Florida Institute of Technology, Melbourne, Florida 32901, USA
¹⁹Florida State University, Tallahassee, Florida 32306, USA
²⁰Georgia State University, Atlanta, Georgia 30303, USA
²¹Hiroshima University, Kagamiyama, Higashi-Hiroshima 739-8526, Japan
²²IHEP Protvino, State Research Center of Russian Federation, Institute for High Energy Physics, Protvino, 142281, Russia
²³University of Illinois at Urbana-Champaign, Urbana, Illinois 61801, USA
²⁴Institute for Nuclear Research of the Russian Academy of Sciences, prospekt 60-letiya Oktyabrya 7a, Moscow 117312, Russia
²⁵Institute of Physics, Academy of Sciences of the Czech Republic, Na Slovance 2, 182 21 Prague 8, Czech Republic
²⁶Iowa State University, Ames, Iowa 50011, USA
²⁷Joint Institute for Nuclear Research, 141980 Dubna, Moscow Region, Russia
²⁸Helsinki Institute of Physics and University of Jyväskylä, P.O. Box 35, FI-40014 Jyväskylä, Finland
²⁹KEK, High Energy Accelerator Research Organization, Tsukuba, Ibaraki 305-0801, Japan
³⁰Korea University, Seoul, 136-701, Korea
³¹Russian Research Center "Kurchatov Institute," Moscow, 123098 Russia
³²Kyoto University, Kyoto 606-8502, Japan
³³Laboratoire Leprince-Ringuet, Ecole Polytechnique, CNRS-IN2P3, Route de Saclay, F-91128, Palaiseau, France
³⁴Lawrence Livermore National Laboratory, Livermore, California 94550, USA
³⁵Los Alamos National Laboratory, Los Alamos, New Mexico 87545, USA
³⁶LPC, Université Blaise Pascal, CNRS-IN2P3, Clermont-Fd, 63177 Aubiere Cedex, France
³⁷Department of Physics, Lund University, Box 118, SE-221 00 Lund, Sweden
³⁸University of Maryland, College Park, Maryland 20742, USA
³⁹Department of Physics, University of Massachusetts, Amherst, Massachusetts 01003-9337, USA
⁴⁰Institut für Kernphysik, University of Muenster, D-48149 Muenster, Germany
⁴¹Muhlenberg College, Allentown, Pennsylvania 18104-5586, USA
⁴²Myongji University, Yongin, Kyonggido 449-728, Korea
⁴³Nagasaki Institute of Applied Science, Nagasaki-shi, Nagasaki 851-0193, Japan
⁴⁴University of New Mexico, Albuquerque, New Mexico 87131, USA
⁴⁵New Mexico State University, Las Cruces, New Mexico 88003, USA
⁴⁶Oak Ridge National Laboratory, Oak Ridge, Tennessee 37831, USA
⁴⁷IPN-Orsay, Université Paris Sud, CNRS-IN2P3, BP1, F-91406, Orsay, France
⁴⁸Peking University, Beijing 100871, People's Republic of China
⁴⁹PNPI, Petersburg Nuclear Physics Institute, Gatchina, Leningrad region, 188300, Russia
⁵⁰RIKEN Nishina Center for Accelerator-Based Science, Wako, Saitama 351-0198, Japan
⁵¹RIKEN BNL Research Center, Brookhaven National Laboratory, Upton, New York 11973-5000, USA
⁵²Physics Department, Rikkyo University, 3-34-1 Nishi-Ikebukuro, Toshima, Tokyo 171-8501, Japan
⁵³Saint Petersburg State Polytechnic University, St. Petersburg, 195251 Russia
⁵⁴Universidade de São Paulo, Instituto de Física, Caixa Postal 66318, São Paulo CEP05315-970, Brazil
⁵⁵Seoul National University, Seoul, Korea
⁵⁶Chemistry Department, Stony Brook University, SUNY, Stony Brook, New York 11794-3400, USA
⁵⁷Department of Physics and Astronomy, Stony Brook University, SUNY, Stony Brook, New York 11794-3400, USA

⁵⁸*University of Tennessee, Knoxville, Tennessee 37996, USA*⁵⁹*Department of Physics, Tokyo Institute of Technology, Oh-okayama, Meguro, Tokyo 152-8551, Japan*⁶⁰*Institute of Physics, University of Tsukuba, Tsukuba, Ibaraki 305, Japan*⁶¹*Vanderbilt University, Nashville, Tennessee 37235, USA*⁶²*Waseda University, Advanced Research Institute for Science and Engineering, 17 Kikui-cho, Shinjuku-ku, Tokyo 162-0044, Japan*⁶³*Weizmann Institute, Rehovot 76100, Israel*⁶⁴*Institute for Particle and Nuclear Physics, Wigner Research Centre for Physics, Hungarian Academy of Sciences (Wigner RCP, RMKI) H-1525 Budapest 114, PO Box 49, Budapest, Hungary*⁶⁵*Yonsei University, IPAP, Seoul 120-749, Korea*

(Received 21 August 2011; published 19 September 2012)

The second Fourier component v_2 of the azimuthal anisotropy with respect to the reaction plane is measured for direct photons at midrapidity and transverse momentum (p_T) of 1–12 GeV/ c in Au + Au collisions at $\sqrt{s_{NN}} = 200$ GeV. Previous measurements of this quantity for hadrons with $p_T < 6$ GeV/ c indicate that the medium behaves like a nearly perfect fluid, while for $p_T > 6$ GeV/ c a reduced anisotropy is interpreted in terms of a path-length dependence for parton energy loss. In this measurement with the PHENIX detector at the Relativistic Heavy Ion Collider we find that for $p_T > 4$ GeV/ c the anisotropy for direct photons is consistent with zero, which is as expected if the dominant source of direct photons is initial hard scattering. However, in the $p_T < 4$ GeV/ c region dominated by thermal photons, we find a substantial direct-photon v_2 comparable to that of hadrons, whereas model calculations for thermal photons in this kinematic region underpredict the observed v_2 .

DOI: [10.1103/PhysRevLett.109.122302](https://doi.org/10.1103/PhysRevLett.109.122302)

PACS numbers: 25.75.Dw

Direct photons are produced in various processes during the entire space-time history of relativistic heavy ion collisions and, due to their small coupling, can leave the collision region without appreciable further interaction. This makes them a sensitive and direct probe of all stages of the collision, including initial hard scattering, formation, and evolution of the strongly interacting partonic medium, its transition to hadronic matter, and final decoupling [1,2]. The transverse momentum (p_T) ranges populated by various production mechanisms overlap. However, azimuthal asymmetries tied to the event-by-event collision geometry provide useful additional information and a means to distinguish between sources of direct photons. In this Letter we consider the second Fourier component (v_2 , often referred to as elliptic flow) of the event-by-event photon distribution in azimuth with respect to the reaction plane in Au + Au collisions at 200 GeV.

At higher p_T (> 4 GeV/ c) there are four fundamental sources of direct photons, characterized by different v_2 [2,3]. Photons from initial hard scattering (predominantly from $qg \rightarrow q\gamma$ “gluon Compton scattering”) are isotropic and so $v_2 = 0$. Jet-fragmentation photons have positive v_2 since the energy loss of the originating parton is smaller in the reaction plane [4]. Jet-conversion photons, where a hard-scattered quark interacts with a thermal gluon in the medium and converts into a photon with almost equal p_T have negative v_2 [3], because the average path length of the parton in the medium (proportional to the conversion probability) is larger out of the reaction plane than within. Finally, Bremsstrahlung photons are also emitted preferentially in the direction where the medium is thicker, leading to a negative v_2 [3]. Note that in this picture the azimuthal asymmetry of high- p_T photon

production—while expressed in terms of v_2 —reflects the pure geometry of the medium, not its dynamics; it depends on the path length, not on the boost from the hydrodynamic pressure gradients.

The picture is quite different in the low- p_T range ($1 < p_T < 4$ GeV/ c), which is dominated by thermal photons (as first measured in [5]), where bulk dynamics (expansion) plays an important role, since it influences both the rate and azimuthal asymmetries of photon production [3,6]. It is now established that collectivity—which already exists in the partonic phase (strongly interacting quark-gluon plasma, sQGP)—persists after transition into the hadronic phase and the resulting azimuthal asymmetries in particle production can be described by nearly ideal hydrodynamics. The expectation is that thermal radiation from both the sQGP and the hadronic phase will inherit the collective motion of the medium, i.e., will have a bona-fide elliptic flow, positive v_2 at low p_T [7]. The low- p_T behavior of direct-photon v_2 puts constraints on the viscosity of the sQGP [6].

The PHENIX experiment has published the invariant-yield as a function of p_T for direct photons both via real photons and internal conversions of nearly-real virtual photons [5,8]. In the $1 < p_T < 4$ GeV/ c region, a substantial excess of direct photons was observed relative to scaling of $p + p$ yields and was interpreted in terms of thermal photon emission from the hot medium. An early attempt to infer v_2 of direct photons from a π^0 and inclusive-photon- v_2 measurement performed in a limited p_T range was published in [9].

In this Letter, we present measurements by the PHENIX experiment [10] of v_2 of π^0 and inclusive photons in a much-extended p_T range (up to 12 GeV/ c) in

$\sqrt{s_{NN}} = 200$ GeV Au + Au collisions. Also, at low p_T the fraction R_γ of direct over inclusive photons is now measured with much higher precision [5] than before [8]. Therefore, for the first time a meaningful extraction of the direct-photon v_2 itself is possible.

The data are from the 2007 run of the Relativistic Heavy Ion Collider at Brookhaven National Laboratory. The analyzed sample includes $\sim 3.0 \times 10^9$ minimum-bias Au + Au collisions. Events are triggered by the beam-beam counters (BBC), as described in [11], which comprise two arrays of Čerenkov counters covering $3.1 < |\eta| < 3.9$ and 2π in azimuth in both beam directions. Event centrality is determined by the charge sum in the BBC.

The event-by-event reaction plane (RP) is determined by two types of detectors, the first being the BBC itself. The RP resolution (effectively a dilution factor with which the observed v_2 is normalized to obtain the true v_2) is defined as $\sigma_{RP} = \langle \cos[2(\Psi^{\text{true}} - \Psi^{\text{RP}})] \rangle$ and it is established by comparing event-by-event the RPs obtained separately in the two BBCs. The resolution is best in the 20%–30% centrality bin, where it reaches a value of 0.4. For the 2007 data taking period, a dedicated reaction-plane detector (RXN) [12] covers $1.0 < |\eta| < 2.8$ and the full azimuth. The RXN is a highly segmented lead-scintillator sampling detector providing much better measurement ($\sigma_{RP} \sim 0.7$) than the BBC, but it is closer to the central $|\eta| < 0.35$ pseudorapidity region where v_2 is measured, making it more sensitive to jet bias in those (rare) events, where a high- p_T particle is observed. The $0.7/0.4 = 1.75$ improvement on the reaction-plane resolution is a 1.75-fold improvement on point-by-point uncertainty.

Inclusive photons are measured in the PHENIX electromagnetic calorimeter [13]. Particles are identified (PID) and hadrons are rejected by a shower-shape cut and a veto on charged particles using the pad chambers [14]. Photons in each p_T range are binned according to $\Phi - \Psi^{\text{RP}}$, where Ψ^{RP} is the azimuth of the event-by-event reaction plane, which is established independently by the BBC and RXN. These distributions are then fit for each p_T range with $N_0[1 + 2v_2 \cos\{2(\Phi - \Psi^{\text{RP}})\}]$ to extract the raw $v_2^{\gamma, \text{meas}}$

coefficient for inclusive photons. As a cross-check of the fit value, another $v_2^{\gamma, \text{meas}}$ is also calculated from the average cosine of the particles with respect to the reaction plane.

Two sources of background to direct photons are of concern—hadronic decay photons and charged hadrons surviving the photon ID cuts. The cuts eliminate virtually all hadrons above 6 GeV deposited energy, which may arise from hadrons of any p_T above 6 GeV/c. However, some lower p_T hadrons survive the cuts. We correct for the v_2 of this contamination, and cross check the result using conversion photons detected as dielectrons, which are free of hadron contamination [15].

To correct for hadron contamination, pions, kaons, and protons are simulated using GEANT [16], including the calorimeter response. The fraction of charged hadrons in the sample surviving the photon ID cuts is determined as $N^{\text{hadr}}/N^{\text{meas}}$. The total hadron contamination is typically 20% at 2 GeV energy deposited in the calorimeter, 10% at 4 GeV, and negligible above 6 GeV. The weighted sum of these contributions is combined into a single v_2^{hadr} using the range of hadron p_T corresponding to each bin of deposited energy. A maximum v_2 of 0.18 is reached at 2 GeV. The corrected value of inclusive photons is then obtained using

$$v_2^{\gamma, \text{obs}} = \frac{v_2^{\gamma, \text{meas}} - (N^{\text{hadr}}/N^{\text{meas}})v_2^{\text{hadr}}}{1 - N^{\text{hadr}}/N^{\text{meas}}}. \quad (1)$$

Since v_2^{hadr} is very similar to $v_2^{\gamma, \text{meas}}$, the largest difference $v_2^{\gamma, \text{meas}} - v_2^{\gamma, \text{obs}}$ introduced by Eq. (1) is $0.15 - (0.15 - [0.2 \times 0.18])/0.8 = 0.0075$, or 5% of $v_2^{\gamma, \text{meas}}$. The uncertainty of this correction (see Table I) is estimated by replacing the individual charged-hadron spectra with only charged pions, and then repeating the procedure. Finally, the true v_2 for inclusive photons is obtained from $v_2^{\gamma, \text{inc}} = v_2^{\gamma, \text{obs}}/\sigma_{RP}$. A large fraction of inclusive photons comes from hadron decays, predominantly from π^0 ($\sim 80\%$) and η ($\sim 15\%$), with a small fraction coming from ρ , ω , and η' decays, but only the π^0 v_2 is directly measured. The measurement of neutral pions and their v_2 is described in detail in [4, 17]. We assume that η , ω , etc., follow the same KE_T

TABLE I. Typical systematic uncertainties ($\delta x/x$) contributing to the direct-photon $v_2^{\gamma, \text{dir}}$ measurement for minimum-bias collisions over two p_T ranges, and absolute uncertainty of $v_2^{\gamma, \text{dir}}$. Note that the uncertainty of $v_2^{\gamma, \text{dir}}$ is not the simple linear or quadratic sum of the uncertainties listed, but is derived by differentiation from the above expression on $v_2^{\gamma, \text{dir}}$. The last row shows this absolute uncertainty.

Contributing via	Source	p_T range 1–3	(GeV/c) 10–12	Type
$v_2^{\gamma, \text{inc}}$	Remaining hadrons	0.022		<i>B</i>
	v_2 extraction method	0.004	0.006	<i>B</i>
$v_2^{\pi^0}$	Particle ID	0.037	0.06	<i>B</i>
	Normalization	0.004	0.072	<i>B</i>
	Shower merging		0.04	<i>B</i>
Subtraction	R_γ	0.031	0.22	<i>A</i>
Common	Reaction plane	0.063	0.063	<i>C</i>
Absolute uncertainty of $v_2^{\gamma, \text{dir}}$		0.07	0.02	

scaling observed in hadrons [18], where $KE_T = m_T - m$. Thus, $v_2^{\text{hadr}}(p_T)$ can be calculated for all hadrons separately from $v_2^{\pi^0}(p_T)$ and then combined. As in [5], we assume m_T scaling of hadron p_T spectra and establish a ‘‘hadron cocktail’’ using the measured yield ratios. This cocktail is the input of a Monte Carlo simulation to calculate the combined $v_2^{\gamma,\text{bg}}$ due to photons from hadron decays. The direct-photon $v_2^{\gamma,\text{dir}}$ is then obtained using the $R_\gamma(p_T)$ ‘‘direct-photon-excess ratio’’ as

$$v_2^{\gamma,\text{dir}} = \frac{R_\gamma(p_T)v_2^{\gamma,\text{inc}} - v_2^{\gamma,\text{bg}}}{R_\gamma(p_T) - 1} = v_2^{\gamma,\text{inc}} + \frac{v_2^{\gamma,\text{inc}} - v_2^{\gamma,\text{bg}}}{R_\gamma(p_T) - 1}, \quad (2)$$

where $R_\gamma(p_T) = N^{\text{inc}}(p_T)/N^{\text{bg}}(p_T)$ with $N^{\text{inc}} = N^{\text{meas}} - N^{\text{hadr}}$, the number of inclusive photons, while $N^{\text{bg}}(p_T)$ is the number of photons attributed to hadron decay. Values of $R_\gamma(p_T)$ above 5 GeV/c are taken from the real-photon measurement with the PHENIX electromagnetic calorimeter [8], and below that from the more accurate, but p_T -range-limited internal-conversion measurement of direct photons [5]. Note that $(R_\gamma - 1)$ is measured with a relative uncertainty of 20% at low p_T . Even though the excess is small in this range ($\approx 20\%$), the $v_2^{\gamma,\text{inc}} - v_2^{\gamma,\text{bg}}$ in Eq. (2) is of the order of 0.01 [see Fig. 1(b)], yielding only a small overall correction term.

Contributors to systematic uncertainties for representative p_T values are listed in Table I. The total uncertainty is then derived by differentiating the formula on $v_2^{\gamma,\text{dir}}$ and using the $\delta x/x$ values listed in Table I. Type A are point-by-point uncertainties, which are uncorrelated with p_T ; type B are uncertainties, which are correlated (with p_T); and type C is the overall normalization uncertainty, moving all points by the same fraction up or down. Since the v_2 measurement is relative (the azimuthal anisotropy is fit without the need to know the absolute normalization), the π^0 and inclusive-photon- v_2 measurements are largely immune to energy-scale uncertainties, which are typically the dominant source of uncertainty in an absolute (invariant-yield) measurement. The uncertainties on v_2 are dominated by the common uncertainty on determining σ_{RP} and by uncertainties in particle identification. Uncertainties from absolute yields enter indirectly via the hadron cocktail (normalization) and more directly at higher p_T (where the real-photon measurement is used) by the $R_\gamma(p_T)$ needed to establish the direct-photon v_2 . Note that due to the way $v_2^{\gamma,\text{dir}}$ is calculated, once R_γ is large, its relative uncertainty contributes to the uncertainty on $v_2^{\gamma,\text{dir}}$ less and less.

Figure 1 shows steps of the analysis using the minimum-bias sample, as well as the differences between results obtained with BBC and RXN. First, v_2 of π^0 and inclusive photons ($v_2^{\pi^0}$, $v_2^{\gamma,\text{inc}}$) are measured, as described above [panels (a) and (b)]. Then, using the $v_2^{\gamma,\text{bg}}$ of photons from hadronic decays and the R_γ direct-photon excess

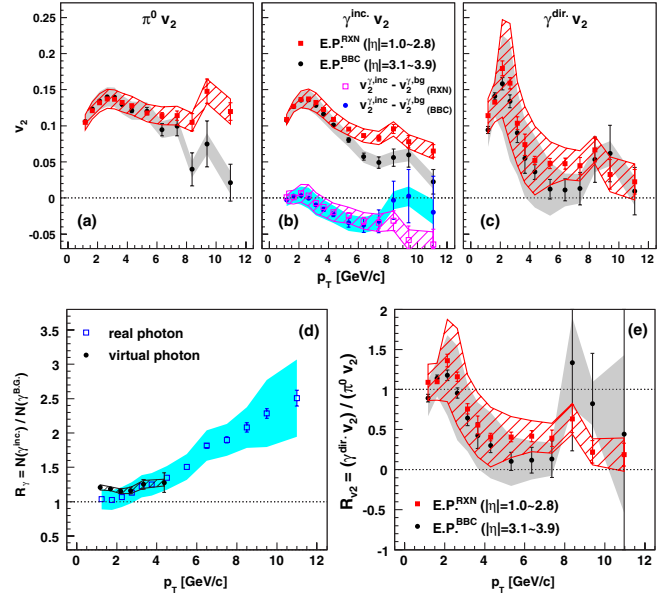


FIG. 1 (color online). (a)–(c) v_2 in minimum-bias collisions, using two different reaction-plane detectors: (solid black circles) BBC and (solid red squares) RXN for (a) π^0 , (b) inclusive photon, and (c) direct photon. (d) direct-photon fraction R_γ for (solid-black circles) virtual photons [5] and (open-blue squares) real photons [8] and (e) ratio of direct-photon to π^0 v_2 for (solid-black circles) BBC and (solid-red squares) RXN. The vertical error bars on each data point indicate statistical uncertainties and shaded (gray and cyan) and hatched (red) areas around the data points indicate sizes of systematic uncertainties. On panel (b) the difference of $v_2^{\gamma,\text{inc}}$ and $v_2^{\gamma,\text{bg}}$ is also shown.

ratio, we derive the $v_2^{\gamma,\text{dir}}$ of direct photons [panel (c)]. Panel (d) shows the $R_\gamma(p_T)$ values from the direct-photon invariant-yield measurements using internal conversion [5] and real [8] photons, with their respective uncertainties. Panel (e) shows the ratio of $v_2^{\gamma,\text{dir}}/v_2^{\pi^0}$. We observe substantial direct-photon flow in the low- p_T region (c), commensurate with the hadron flow itself (e). However, in contrast to hadrons, the direct-photon v_2 rapidly decreases with p_T , and for $p_T \geq 5$ GeV/c, it is consistent with zero (c). The rapid transition from large direct-photon flow at 3 GeV/c to zero flow at 5 GeV/c is also demonstrated on panel (e), since the π^0 v_2 changes little in this region [4].

The surprising result that at low- p_T $v_2^{\gamma,\text{dir}}$ is quite large with relatively small uncertainty hinges upon two facts. On the one hand, $v_2^{\gamma,\text{inc}}$ is virtually equal to $v_2^{\gamma,\text{bg}}$ with small uncertainty, as shown on panel (b) of Fig. 1 (note that the uncertainty on their difference is small since it is dominated by the common reaction-plane uncertainty). On the other hand, $R_\gamma(p_T)$ is larger than 1.0 with small uncertainty [5]; these combine to make the second term in Eq. (2) small, also with small uncertainty.

A major issue in any azimuthal-asymmetry measurement is the potential bias from where in pseudorapidity the (event-by-event) reaction plane is measured. At low

p_T —where multiplicities are high and particle production is dominated by the bulk with genuine hydrodynamic behavior—there is no difference between the flow derived with BBC and RXN. However, at higher p_T we observe that the v_2 values using BBC and RXN diverge less for inclusive photons, particularly for π^0 [panel (a) in Fig. 1]. For direct photons [panel (c)], the two results are apparently consistent within their *total* uncertainty, including the uncertainty $\delta R_\gamma/R_\gamma$ (see Table I). However, R_γ is a common correction factor in the v_2 measurements with both reaction-plane detectors.

Event substructure not related to bulk properties and expansion—most notably jets—can bias the reaction-plane measurement, particularly at higher p_T and lower multiplicity. Observation of a high- p_T particle practically guarantees the presence of a jet, which in turn modifies the event structure over a large η range. The bias on the true event plane (with the bulk as its origin) is stronger if the overall multiplicity is small and if the η gap between the central arm (where v_2 is measured) and the reaction-plane detector is reduced. The bias in Fig. 1 is largest for π^0 , since high- p_T hadrons are always jet fragments. Inclusive photons are a mixture of hadron decay photons, inheriting the bias seen in π^0 and the mostly unbiased direct photons, therefore, the difference between BBC and RXN is smaller. Finally, the bias is smallest (but nonzero) for direct photons, of which only a relatively small fraction (jet-fragmentation photons) exhibit bias.

Figure 2 shows v_2 for minimum-bias collisions and two centrality bins versus p_T for π^0 , inclusive photons, and direct photons. For reaction-plane determination the BBC is used because it is farthest from midrapidity where v_2 is measured. Despite the fact that there is a significant direct (thermal) photon yield at low p_T [5], the π^0 and inclusive-photon v_2 is virtually identical there. Note that the surprisingly large inclusive-photon v_2 is confirmed by the (so far preliminary) results with a completely different analysis technique [15]. For direct photons at low p_T we observe a pronounced positive $v_2^{\gamma,\text{dir}}$ signal, increasing with decreasing centrality and comparable to the π^0 flow, but then rapidly going toward zero at 5–6 GeV/c. Qualitatively this shape is similar to the prediction for very early thermalization times, 0.4–0.6 fm/c in [19], namely, the p_T where $v_2^{\gamma,\text{dir}}$ reaches its maximum is consistent with our measurement [see panel (d) in Fig. 2], but its calculated magnitude is too small. The situation is similar for the calculation with $\tau_0 = 0.2$ fm/c and vanishing viscosity in [7]. The model in [20] combines somewhat later thermalization time (0.6 fm/c) with partial chemical equilibrium in the hadronic phase, reproducing the shape, but still predicts smaller $v_2^{\gamma,\text{dir}}$ at low p_T than the observed one. While such large direct-photon v_2 could be attributed in principle to a dominant production mechanism at the later stage when bulk flow is already developed [21,22], simultaneously explaining the large values of $v_2^{\gamma,\text{dir}}$ at ~ 2 GeV/c and its vanishing above 5 GeV/c remains a challenge to current

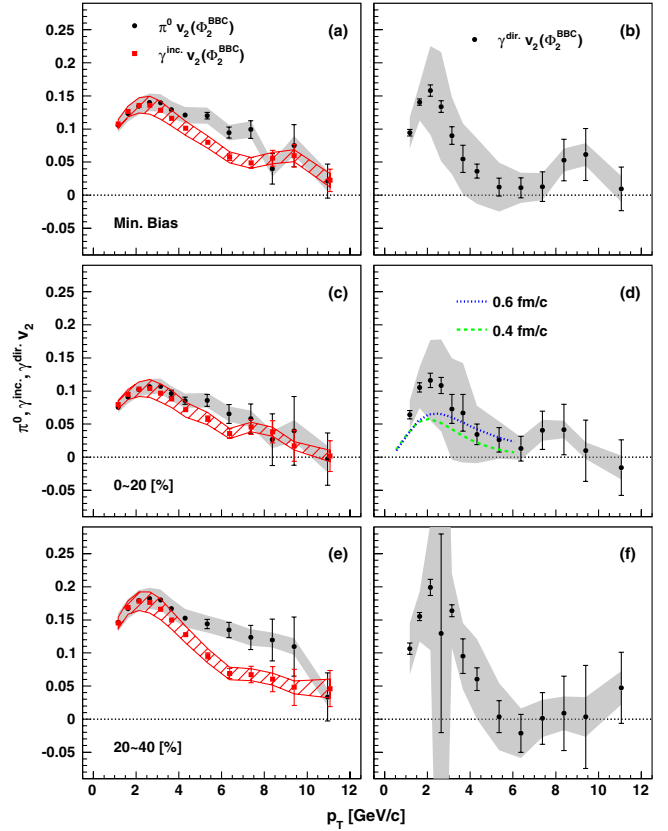


FIG. 2 (color online). (a),(c),(e) Centrality dependence of v_2 for (solid-black circles) π^0 , (solid-red squares) inclusive photons, and (b),(d),(f) (solid-black circles) direct photons measured with the BBC detector for (a),(b) minimum-bias (c),(d) 0%–20% centrality, and (e),(f) 20%–40% centrality. For (b),(d),(f) the direct-photon fraction is taken from [5] up to 4 GeV/c and from [8] for higher p_T . The vertical error bars on each data point indicate statistical uncertainties and the shaded (gray) and hatched (red) areas around the data points indicate sizes of systematic uncertainties. Also shown on panel (d) are two calculations from [19] using two different τ_0 initial times: 0.6 fm/c (upper curve) and 0.4 fm/c (lower curve).

theories (see, for instance, a recent model comparison to the current data in Fig. 5 of [22]).

Figure 3 shows the high- p_T integrated v_2 ($p_T > 6$ GeV/c) for π^0 and photons (inclusive and direct) as a function of centrality. The low- N_{part} behavior is strongly influenced by the location in pseudorapidity of the reaction-plane detector. The π^0 v_2 is comparable to other hadrons and is higher than the inclusive-photon v_2 , which is diluted by direct photons. The two direct-photon- v_2 measurements [panel (c)] are consistent with zero (and each other) at all centralities within their total systematic uncertainties. While zero $v_2^{\gamma,\text{dir}}$ would be expected if initial hard scattering is the dominant (sole considered) source of photons, the typical contribution from jet conversion only is $v_2^{\gamma,\text{dir}} \sim -0.02$ and from fragmentation is $v_2^{\gamma,\text{dir}} \leq 0.01$, weighted with the fraction of photons coming from these

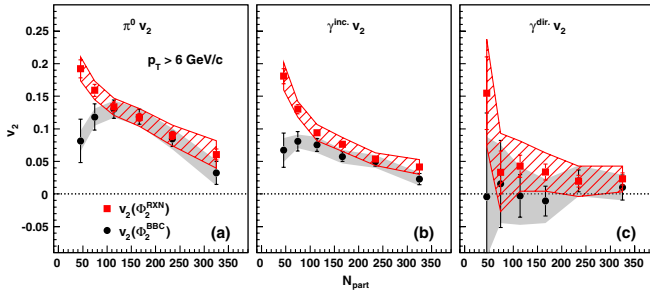


FIG. 3 (color online). High- p_T ($p_T > 6$ GeV/ c) integrated v_2 vs N_{part} for (a) π^0 , (b) inclusive photon, and (c) direct photon. Results are shown with both reaction-plane detectors: (solid-black circles) BBC and (solid-red squares) RXN. Each point represents a 10% wide centrality bin from 60%–0%. The vertical error bars on each data point indicate statistical uncertainties and the shaded (gray) and hatched (red) areas around the data points indicate sizes of systematic uncertainties.

specific processes [3,7]. Currently the experiment is not sensitive to their negative/positive contributions to $v_2^{\gamma,\text{dir}}$.

In conclusion, we measured v_2 of π^0 , inclusive and direct photons in the $1 < p_T < 12$ GeV/ c range for minimum bias and selected centralities in $\sqrt{s_{NN}} = 200$ GeV Au + Au collisions. At higher p_T (> 6 GeV/ c) the direct-photon v_2 is consistent with zero at all centralities, as expected if the dominant source of photon production is initial hard scattering. However, the experimental uncertainties are currently about a factor of 2 higher than the predicted (small) positive and negative contributions from fragmentation and jet-conversion photons, respectively. In the thermal region ($p_T < 4$ GeV/ c), a positive direct-photon v_2 is observed, which is comparable in magnitude to the π^0 v_2 and consistent with early thermalization times and low viscosity.

We thank the staff of the Collider-Accelerator and Physics Departments at Brookhaven National Laboratory and the staff of the other PHENIX participating institutions for their vital contributions. We acknowledge support from the Office of Nuclear Physics in the Office of Science of the Department of Energy, the National Science Foundation, Abilene Christian University Research Council, Research Foundation of SUNY, and Dean of the College of Arts and Sciences, Vanderbilt University (U.S.), Ministry of Education, Culture, Sports, Science, and Technology and the Japan Society for the Promotion of Science (Japan), Conselho Nacional de Desenvolvimento Científico e Tecnológico and Fundação de Amparo à Pesquisa do Estado de São Paulo (Brazil), Natural Science Foundation of China (P. R. China), Ministry of Education, Youth and Sports (Czech Republic), Centre National de la Recherche Scientifique, Commissariat à l'Énergie Atomique, and Institut National de Physique Nucléaire et de Physique des Particules (France), Bundesministerium für Bildung und Forschung, Deutscher Akademischer Austausch Dienst, and Alexander von Humboldt Stiftung (Germany), Hungarian National Science Fund, OTKA (Hungary),

Department of Atomic Energy and Department of Science and Technology (India), Israel Science Foundation (Israel), National Research Foundation and WCU program of the Ministry Education Science and Technology (Korea), Ministry of Education and Science, Russian Academy of Sciences, Federal Agency of Atomic Energy (Russia), VR and the Wallenberg Foundation (Sweden), the U.S. Civilian Research and Development Foundation for the Independent States of the Former Soviet Union, the U.S.-Hungarian Fulbright Foundation for Educational Exchange, and the U.S.-Israel Binational Science Foundation.

*Deceased.

†PHENIX Spokesperson.

jacak@skipper.physics.sunysb.edu

- [1] S. Turbide, R. Rapp, and C. Gale, *Phys. Rev. C* **69**, 014903 (2004).
- [2] W. Liu and R. J. Fries, *Phys. Rev. C* **77**, 054902 (2008).
- [3] S. Turbide, C. Gale, and R. J. Fries, *Phys. Rev. Lett.* **96**, 032303 (2006).
- [4] S. Afanasiev *et al.* (PHENIX Collaboration), *Phys. Rev. C* **80**, 054907 (2009).
- [5] A. Adare *et al.* (PHENIX Collaboration), *Phys. Rev. Lett.* **104**, 132301 (2010).
- [6] K. Dusling, *Nucl. Phys.* **A839**, 70 (2010).
- [7] C. Gale, *Selective Tracer Signals of the QCD Plasma State*, edited by R. Stock (Springer-Verlag, Berlin, Heidelberg, 2010), Vol. 23, p. 445, http://www.springermaterials.com/docs/info/978-3-642-01539-7_15.html.
- [8] S. S. Adler *et al.* (PHENIX Collaboration), *Phys. Rev. Lett.* **94**, 232301 (2005).
- [9] S. S. Adler *et al.* (PHENIX Collaboration), *Phys. Rev. Lett.* **96**, 032302 (2006).
- [10] K. Adcox *et al.*, *Nucl. Instrum. Methods Phys. Res., Sect. A* **499**, 469 (2003).
- [11] M. Allen *et al.* (PHENIX Collaboration), *Nucl. Instrum. Methods Phys. Res., Sect. A* **499**, 549 (2003).
- [12] E. Richardson *et al.* (PHENIX Collaboration), *Nucl. Instrum. Methods Phys. Res., Sect. A* **636**, 99 (2011).
- [13] L. Aphecetche *et al.* (PHENIX Collaboration), *Nucl. Instrum. Methods Phys. Res., Sect. A* **499**, 521 (2003).
- [14] K. Adcox *et al.* (PHENIX Collaboration), *Nucl. Instrum. Methods Phys. Res., Sect. A* **499**, 489 (2003).
- [15] R. Petti, *J. Phys. Conf. Ser.* **316**, 012026 (2011).
- [16] GEANT 3.2.1, CERN Computing Library (1993), <http://wwwasdoc.web.cern.ch/wwwasdoc/pdfdir/geant.pdf>.
- [17] A. Adare *et al.* (PHENIX Collaboration), *Phys. Rev. Lett.* **105**, 142301 (2010).
- [18] A. Adare *et al.* (PHENIX Collaboration), *Phys. Rev. Lett.* **98**, 162301 (2007).
- [19] R. Chatterjee and D. K. Srivastava, *Phys. Rev. C* **79**, 021901(R) (2009).
- [20] F.-M. Liu, T. Hirano, K. Werner, and Y. Zhu, *Phys. Rev. C* **80**, 034905 (2009).
- [21] V. S. Pantuev, [arXiv:1105.4033](https://arxiv.org/abs/1105.4033).
- [22] H. van Hees, C. Gale, and R. Rapp, *Phys. Rev. C* **84**, 054906 (2011).